Analytical Modelling of ATF Chromium-Coated Zr-Based Cladding High Temperature Oxidation in Steam and Steam-Air Atmosphere

Alexander Vasiliev
Nuclear Safety Institute (IBRAE)
B.Tulskaya 52
115191 Moscow, Russia
vasil@ibrae.ac.ru

ABSTRACT

Currently, the comprehension among the specialists and functionaries throughout the world is getting stronger that the nuclear industry can encounter serious difficulties in progress in the case of insufficiently decisive measures to enhance the safety level of nuclear objects and to ensure clean energy and green world. The keen competition with renewable energy sources like wind, solar or geothermal energy takes place presently and is expected to continue in future decades. One of main measures of nuclear safety enhancement could be a drastic renovation of materials used in nuclear industry.

Up to now, several perspective advanced tolerant fuel (ATF) cladding candidates are chosen for possible application in commercial nuclear power plants (NPPs) including zirconium-based cladding with protective chromium coating, which represents more evolutional way in nuclear energy progress.

The analytical model of high-temperature oxidation of *Zr/Cr* cladding is developed based on oxygen diffusion consideration in the cladding. The model necessarily takes into account the initial oxidation of chromium layer with formation of chromium oxide, and, after the loss of its protective properties, the model considers the zirconium oxidation in two- or three-layers configuration. The features of *Zr/Cr* cladding oxidation in the steam-air atmosphere are also discussed. The model is implemented to severe accident computer running code.

The comparison of calculated results for *Zr/Cr* cladding high temperature oxidation with available experimental data is conducted. The reasonable agreement between calculated and experimental data is observed.

The analysis of results obtained allows make the conclusion that the application of chromium-coated *Zr*-based cladding may be optimistic for considerable upgrade of safety level for NPPs especially for design-basis-accident conditions.

1   INTRODUCTION

As a result of theoretical and experimental investigations conducted during recent years, the following materials were determined which are most perspective for use in ATF-claddings [1-8]:
- the chromium-nickel alloys of different compositions;
- the zirconium-based alloys with chromium coating of thickness up to $15 \div 20$ mkm;
- the ceramics *SiC*;
- the alloy *FeCrAl*.

The existing data show that all four materials have parabolic oxidation constants which are one to four orders of magnitude less compared to parabolic constants of standard zirconium-based claddings used currently. This conclusion belongs to design basis accident scenarios with maximum temperatures up to 1200°C.

At the same time, for the normal operation and design-basis accidents the characteristics of fuel and cladding must *get better or remain at the same level*.

Thus, those materials demonstrate exclusively high corrosion resistance and can be considered as perspective candidates for using in the cores of new generation ATF reactors.

At the same time, the experimental studies demonstrate the drastic deterioration of protective properties, considerable increase of hydrogen release and even the total evaporation and degradation for *SiC* when the temperature rises from 1650°C up to 1750°C and higher. The claddings from chromium-nickel alloys have respectively low melting temperature below 1400°C, although possess unique protective properties and exclusively low corrosion rates at lower temperatures. The protective properties of *FeCrAl* claddings sharply diminish when the temperature reaches about 1400°C. Besides that, the lowering of parabolic oxidation coefficient for this material is less considerable (about one order of magnitude compared to Zr-based claddings) among other candidate materials.

The lowering of parabolic oxidation coefficient for Zr-based claddings with chromium coating is considerable (by about two orders of magnitude), also, the positive properties of Zr-based claddings are retained (high melting temperature, low absorption cross-section of thermal neutrons, strong plasticity etc.). These circumstances are probably a good argument in the favor of *Zr/Cr* claddings use in the ATF fuel-cladding system. We can say that possible application of these claddings in commercial nuclear reactors presents more evolutional way of nuclear technology development but not revolution as in the case of application of other new materials.

2   DESCRIPTION OF CHARACTERISTIC PHASES OF ZR/CR CLADDING HIGH TEMPERATURE OXIDATION AND APPROACHES TO MODELLING

The high temperature oxidation of *Zr/Cr* cladding will undergo three characteristic phases:

- chromium oxidation which is characterized by very low parabolic oxidation rate;
- transient phase with progressive growth of oxidation via enhancement of oxygen diffusion rate through both Cr_2O_3 layer (due to spallation and cracks formation in Cr_2O_3 layer) and Cr layer (due to enhanced diffusion along ZrO_2 precipitates grains boundaries);
- basic diffusion in three-layer system $ZrO_2/\alpha\text{-}Zr(O)/\beta\text{-}Zr$ after disappearance of Cr layer and total loss of protective function by Cr_2O_3 layer.

Consecutively all these phases are considered.

2.1   Phase I. Oxidation in a System Zr/Cr

Let us consider high temperature oxidation of chromium plate, see Figure 1. This simple system corresponds to the initial phase of *Zr/Cr* cladding oxidation. Then it is possible to formulate diffusion solution of this problem on the basis of paper [9].
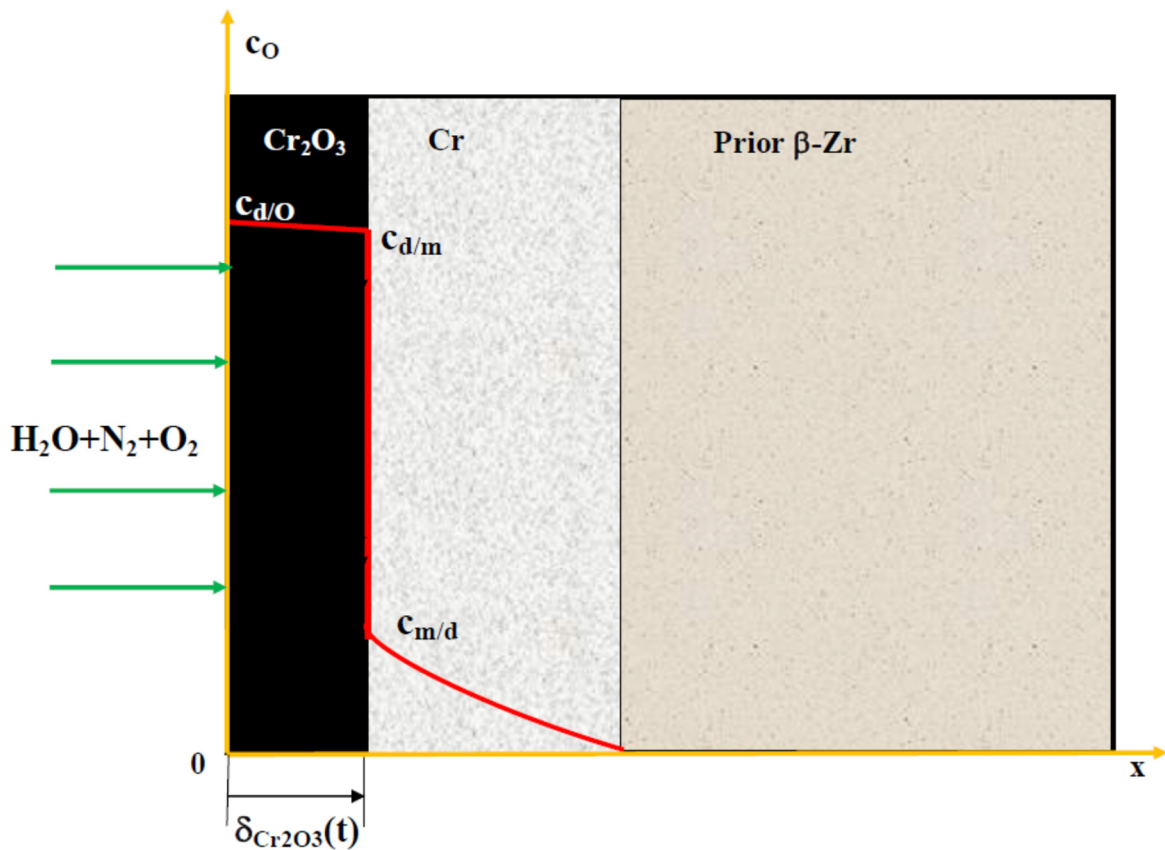
Figure 1: Oxygen concentration profile during phase I

The parabolic kinetics for chromium oxide thickness is represented by

$$\delta_{Cr_2O_3} = \sqrt{k_p t} = K_d\sqrt{t},$$ (1)

$$\frac{K_d}{\sqrt{4D_d}} \cong \frac{\left[\sqrt{\frac{4c_{md}\cdot c_{md}}{\pi} + 8\frac{D_d}{D_m}\left(c_{\frac{d}{m}} - c_{\frac{m}{d}}\cdot r\right)\cdot\left[c_{\frac{d}{O}} - c_{\frac{d}{m}}\right]} - \frac{2c_{\frac{m}{d}}}{\sqrt{\pi}}\right]}{4\sqrt{\frac{D_d}{D_m}}\cdot\left(c_{\frac{d}{m}} - c_{\frac{m}{d}}\cdot r\right)},$$ (2)

where c_O is mass oxygen concentration [kg/m³], K_d – oxidation parabolic constant, D_d and D_m – oxygen diffusion coefficients in Cr_2O_3 and Cr layers respectively, $c_{d/O}$, $c_{d/m} \cong c_{d/O}$ and $c_{m/d}$ – the phase interface concentrations from Cr-O binary phase diagram. The Bedworth-Pilling ratio is equal to $r = \left(\rho_{Cr_2O_3}/\rho_{Cr}\right)\cdot\left(2\mu_{Cr}/\mu_{Cr_2O_3}\right)$. The parameter $c_{m/d}$ is

much less than $c_{d/m}$ because the solubility of oxygen in metallic solid chromium is very low (opposite to oxygen solubility in zirconium) as follows from the literature analysis.

The parabolic constant is approximated by

$$k_p = 4.83 \cdot 10^{-5} \cdot e^{-\frac{31228}{T}} \ \text{m}^2/\text{s} , \tag{3}$$

showing reasonable agreement with the experimental data published in [2].

2.2 Phase II. Transition phase

The gradual worsening of protective properties takes place during this phase. Namely, the effective oxygen diffusion coefficient is enhanced both in the oxide and metallic phases of chromium. It is due to spalling of thin oxide layers and to formation of cracks in the oxide in view of gradual mechanical stress enhancement during oxidation. Also, from experimental observations, see, for example, [2], we can conclude that the formation of intermediate layer *ZrCr₂* (with thickness of about several µm) due to inter-diffusion takes place. Moreover, the atoms of *Zr* diffuse into the metallic chromium coating and form the precipitates of *ZrO₂* after their oxidation [2]. It results in enhancement of effective oxygen diffusion coefficient in chromium layer, because the diffusion is stronger along the grain boundaries.

All these phenomena will lead to gradual enhancement of oxygen flux to metallic zirconium layer resulting in the beginning of its oxidation.
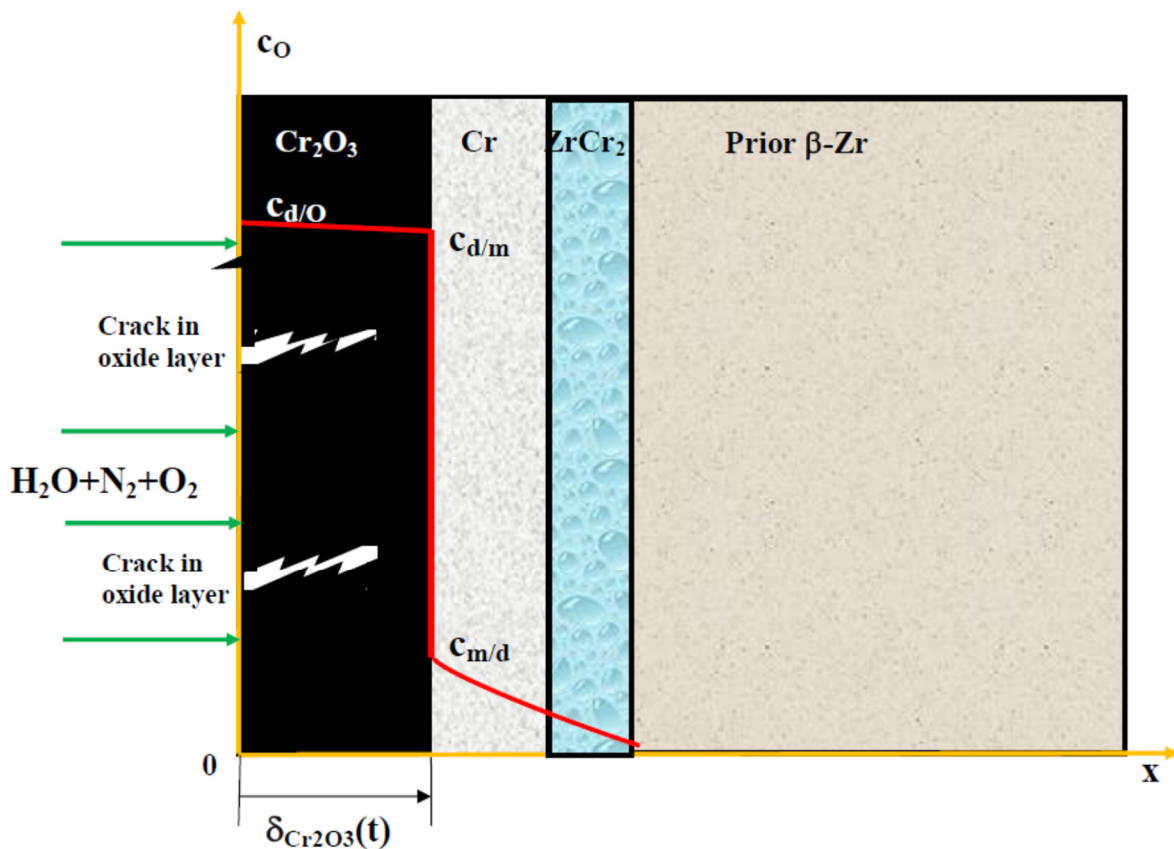

Figure 2: Oxygen concentration profile during phase II

2.3   Phase III. Loss of chromium protective properties

The experiments show that at the stage when the chromium layer has almost disappeared, that is close to fully oxidized state of chromium, the protective properties of both chromium oxide and metallic chromium layers are almost exhausted, see Figure 3. It means that at the phase III we encounter oxidation of Zr-based cladding in a three-layer system ZrO_2+ZrN, α-Zr(O) and β-Zr or in a two-layer configuration ZrO_2 and α-Zr(O) (for lower temperatures) which are well studied. This is why the oxygen diffusion flux through chromium is considerably enhanced now, and it is large enough to ensure initially the growth of α-Zr(O) layer and later of ZrO_2 (or ZrO_2+ZrN layer in the case of steam+air atmosphere). Thus, the full value formation of Zr dioxide layer takes place at this phase due to loss of protective properties of chromium coating.

It seems that more aggressive cladding oxidation is expected in the atmosphere containing nitrogen (steam+air) during this phase compared to oxidation in pure steam. It corresponds to enhancement of effective oxygen diffusion coefficient in porous layer ZrO_2+ZrN.
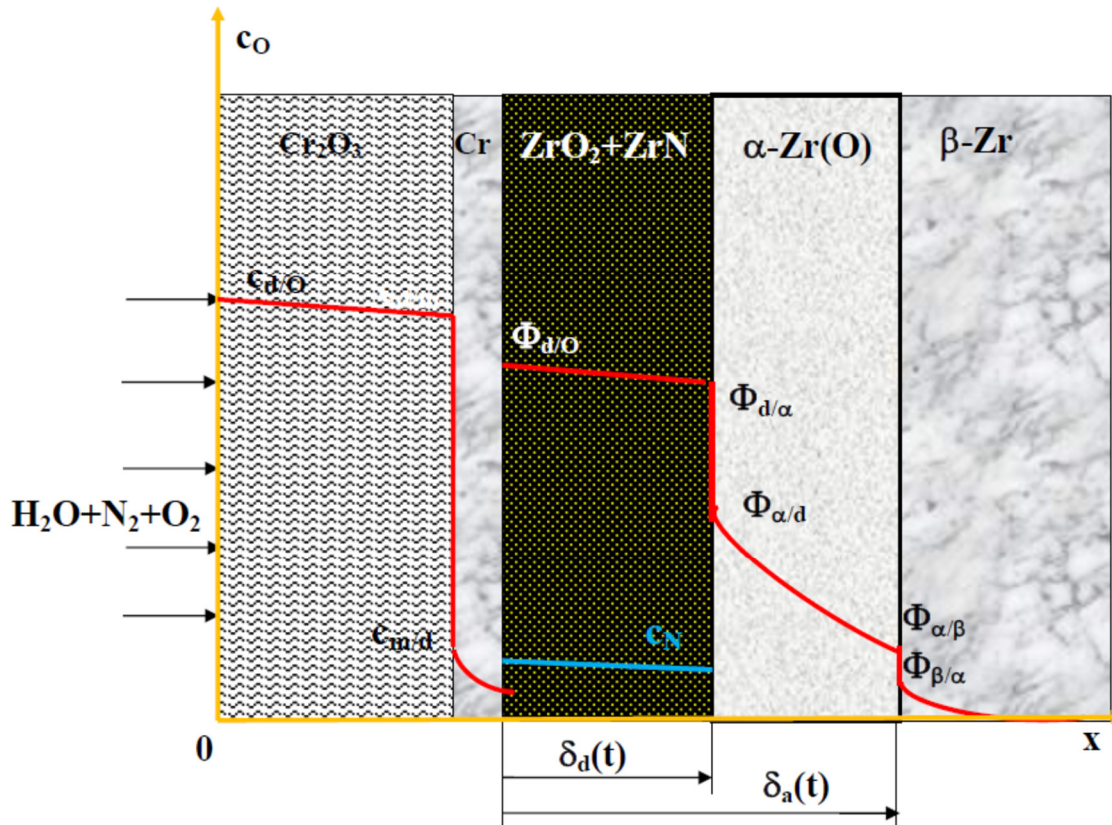

Figure 3: Oxygen concentration profile during phase III. The oxide layer Cr_2O_3 has already lost its protective properties and it is no longer dense as at previous phases I and II.

So, when the protective properties of chromium coating are lost the parabolic kinetics for ZrO_2+ZrN/α-Zr(O) and α-Zr(O)/β-Zr interface coordinates (Figure 3) are represented as

$$\delta_d = K_d\sqrt{t}\,,\ \delta_a = K_a\sqrt{t}\,, \tag{4}$$

$$\frac{K_a}{\sqrt{4D_a}} \cong 1,$$

(5)

$$\frac{K_d}{\sqrt{4D_d}} \cong \frac{-\left(\frac{\Phi_\alpha}{d} - \frac{\Phi_\alpha r}{\beta}\right)\sqrt{\frac{D_a}{D_d}} + \sqrt{\left(\frac{\Phi_\alpha}{d} - \frac{\Phi_\alpha r}{\beta}\right)^2 \frac{D_a}{D_d} + 8A^2\left(\frac{\Phi_d}{\alpha} - \frac{\Phi_\alpha r}{d}\right)\left(\frac{\Phi_d}{O} - \frac{\Phi_d r}{\alpha}\right)}}{4A\left(\frac{\Phi_d}{\alpha} - \frac{\Phi_\alpha r}{d}\right)},$$

$$A = \int_0^{\frac{K_a}{\sqrt{4D_a}}} e^{-y^2} dy.$$

Here r is the Bedworth-Pilling ratio for transition $Zr\text{-}ZrO_2$, Φ - the corresponding interface oxygen concentrations [kg/m^3].

3   ANALYTICAL RESULTS

The analytical approaches described above have been implemented in the numerical code SFPSA developed for description of beyond design basis accidents at NPP spent fuel pools.

Below are presented some results of analytical modelling. Figures 4 and 5 demonstrate parabolic oxidation time dependencies for chromium oxide thickness and cladding weight gain respectively. Despite the reference temperature is high enough (1473 K) the oxide thickness reached only eight μm during 2000 s.
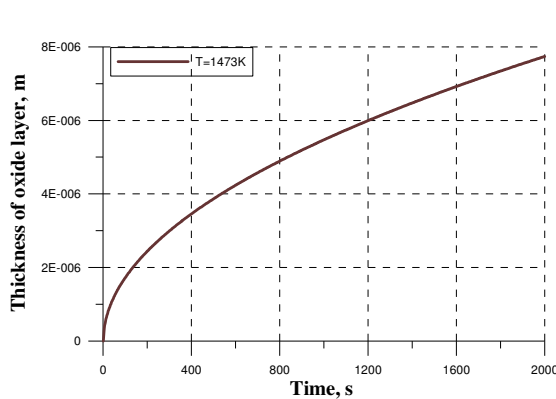

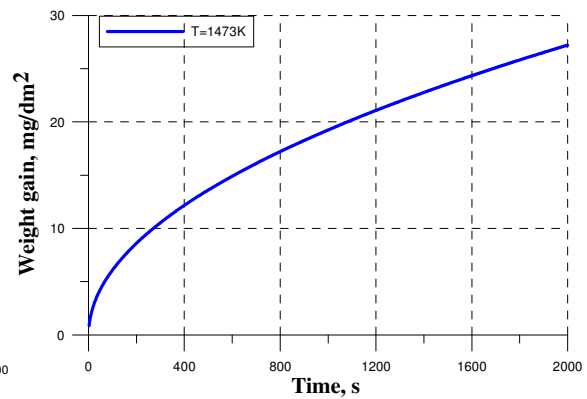Figure 4: Parabolic dependence of Cr_2O_3 thickness on time at T=1473 K

Figure 5: Parabolic dependence of chromium coating weight gain on time at T=1473 K

Figure 6 shows comparison between the cladding weight gain for uncoated and coated claddings. One can note a huge difference in weight gain behaviour between these claddings. We should keep in mind, however, that such extremely low oxidation kinetics for coated sample takes place only during phase I.

The analytical and experimental transition behaviour (phase II) is compared in Figures 7 and 8. The paper [7] is devoted to isothermal oxidation of Zircaloy-4 cladding with Cr coating thickness of about 10 μm at the temperature of 1473K. Figure 7 demonstrates the analytical results derived in this paper for conditions of this experiment. It was supposed in calculations that during the transition phase which is initiated at about time $t=400$ s the effective oxygen diffusion coefficient gradually enhances up to 16 times to time $t=2000$ s. It corresponds to enhancement of parabolic parameter K_d (2) by the factor 4. Such enhancement is enough to reproduce the experimental dependence obtained in the paper [7].
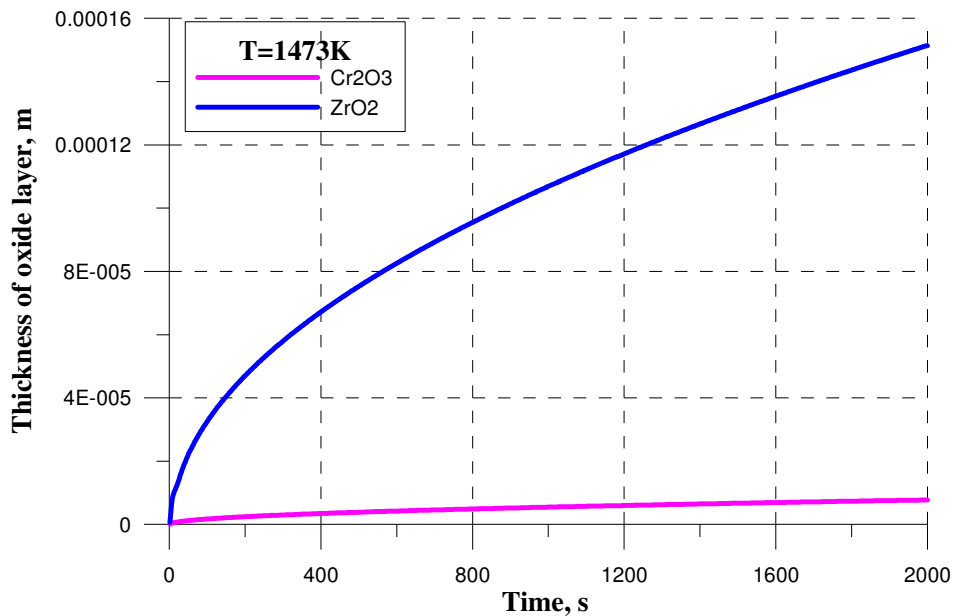

Figure 6: Dynamics of weight gain for uncoated (ZrO_2) and coated cladding (Cr_2O_3) at T=1473K
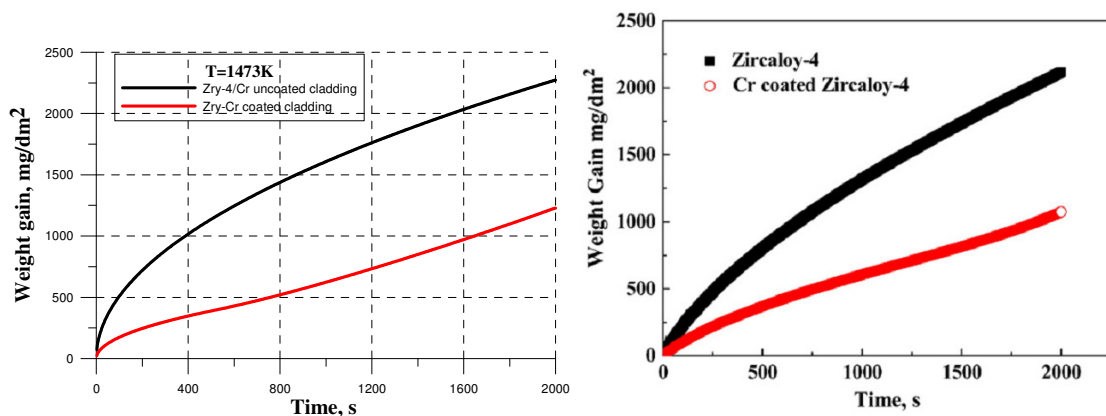

Figure 7: Calculation dynamics of cladding weight gain

Figure 8: Experimental dynamics of cladding weight gain reproduced from the paper [7]

4   CONCLUSIONS

The approaches to model the oxidation of perspective ATF zirconium-based cladding with chromium coating with the thickness up to 15-20 μm were described. The analysis of experimental and analytical results allows one to state that *Zr*-based claddings with chromium coating possess low oxidation kinetics in the temperature range *T*=700÷1300°C. However, three different phases are progressively developing during high temperature oxidation, which result in gradual worsening of oxidation characteristics in the course of oxidation.

Some illustrative results of analytical model developed are given in the paper. They demonstrate the predictive ability of the model.

In the whole, the application of ATF zirconium-based cladding with chromium coating in reactor claddings looks reasonable because of saving time and the possibility of exclusion of accident escalation in the course of severe accident mitigation strategy.

Thus, the most gain from use of *Zr/Cr* claddings is expected for scenarios with temperature range about 700°C-1300°C that is design-basis accident and respectively low hydrogen generation rate is expected. The difference in such parameters as chemical heat generation, hydrogen generation rate and cumulative hydrogen production may reach up to one order of magnitude in favour of chromium-coated claddings compared to standard Zr-based claddings.

ACKNOWLEDGMENTS

REFERENCES

[1]   K.Terrani, "Accident Tolerant Fuel Cladding Development: Promise, Status, and Challenges", J. of Nuclear Materials, 501, 2018, P. 13-30.

[2]   J.-Ch. Brachet, E. Rouesne, J. Ribis, T. Guilbert, S. Urvoy, G. Nony, C. Toffolon-Masclet, M. Le Saux, N. Chaabane, H. Palancher, A. David, J. Bischoff, J. Augereau, E. Pouillier, "High Temperature Steam Oxidation of Chromium-Coated Zirconium-Based Alloys: Kinetics and Process", Corrosion Science, 167, 2020, 108537, 15 pp. Online version: https://doi.org/10.1016/j.corsci.2020.108537.

[3]   P. Vrbka, J. Krejci, J. Kabatova et al., "Air Oxidation of Sponge Based E110 Cladding Alloy at High Temperatures", Proc. 23rd International QUENCH Workshop (QUENCH-23), Karlsruhe, Germany, October 17-19, 2017.

[4]   V. Avincola, "Oxidation and Quench of Silicon Carbide Composites in High Temperature Corrosive Environments", Proc. 20th International QUENCH Workshop (QUENCH-20), Karlsruhe, Germany, November 11-13, 2014.

[5]   M. Steinbrueck, "High-Temperature Oxidation of SiC-Ta-SiC Sandwich Cladding Tubes in GFR Atmosphere", Proc. 22nd International QUENCH Workshop (QUENCH-22), Karlsruhe, Germany, October 18-20, 2016.

[6]   K.G. Field, M.A. Snead, Y. Yamamoto, K.A. Terrani, "Handbook on the Material Properties of FeCrAl Alloys for Nuclear Power Production Applications", ORNL/SPR-2018/905, US, August 2018.

[7]   J.-H. Park, H.-G. Kim, J.-Y. Park, Y.-I. Jung, D.-J. Park, Y.-H. Koo, High Temperature Steam-Oxidation Behavior of Arc Ion Plated Cr Coatings for Accident Tolerant Fuel Claddings", Surface & Coatings Technology, 280, 2015, pp. 256-259.

[8] A. Vasiliev, "High-Temperature Oxidation Modeling of New Perspective Accident Tolerant Fuel Claddings", Proc. 2019 ASME International Mechanical Engineering Congress and Exposition (IMECE2019), Salt Lake City, Utah, US, November 11-14, 2019. IMECE2019-10513.

[9] A. D. Vasiliev. "Advanced Model of Zr-Based Claddings Oxidation in Steam-Oxygen-Nitrogen Gas Mixtures Embracing All Range from Low to High Temperatures", Proc. SAFEST Air Oxidation Meeting "Cladding Oxidation by Air under Severe Accident Conditions in a Nuclear Reactor and a Spent Fuel Pool", Budapest, Hungary, June 14-15, 2016.